


**Please cite the Published Version**

Altarazi, Ahmed, Haider, Julfikar , Alhotan, Abdulaziz, Silikas, Nick and Devlin, Hugh (2023) 3D printed denture base material: the effect of incorporating TiO<sub>2</sub> nanoparticles and artificial ageing on the physical and mechanical properties. *Dental Materials*, 39 (12). pp. 1122-1136. ISSN 0109-5641

**DOI:** <https://doi.org/10.1016/j.dental.2023.10.005>

**Publisher:** Elsevier

**Version:** Published Version

**Downloaded from:** <https://e-space.mmu.ac.uk/632709/>

**Usage rights:**  [Creative Commons: Attribution 4.0](https://creativecommons.org/licenses/by/4.0/)

**Additional Information:** This is an Open Access article which appeared in *Dental Materials*, published by Elsevier

**Enquiries:**

If you have questions about this document, contact [openresearch@mmu.ac.uk](mailto:openresearch@mmu.ac.uk). Please include the URL of the record in e-space. If you believe that your, or a third party's rights have been compromised through this document please see our Take Down policy (available from <https://www.mmu.ac.uk/library/using-the-library/policies-and-guidelines>)



# 3D printed denture base material: The effect of incorporating TiO<sub>2</sub> nanoparticles and artificial ageing on the physical and mechanical properties

Ahmed Altarazi<sup>a,b,\*</sup>, Julfikar Haider<sup>a,c</sup>, Abdulaziz Alhotan<sup>d</sup>, Nick Silikas<sup>a,\*\*</sup>, Hugh Devlin<sup>a</sup>

<sup>a</sup> Division of Dentistry, School of Medical Sciences, University of Manchester, Manchester M13 9PL, United Kingdom

<sup>b</sup> Restorative Dental Science, College of Dentistry, Taibah University, Saudi Arabia

<sup>c</sup> Department of Engineering, Manchester Metropolitan University, Manchester, United Kingdom

<sup>d</sup> Dental Health Department, College of Applied Medical Sciences, King Saud University, Riyadh, Saudi Arabia

## ARTICLE INFO

### Keywords:

3D printed resin  
Titanium dioxide  
Nanoparticles  
Nanocomposite, Stereolithography (SLA)  
Additive manufacturing  
Denture base  
Martens hardness

## ABSTRACT

**Objectives:** To evaluate the physical and mechanical properties of three-dimensional (3D) printed denture base resin incorporating TiO<sub>2</sub> nanoparticles (NPs), subjected to a physical ageing process.

**Methods:** Acrylic denture base samples were prepared by a Stereolithography (SLA) 3D printing technique reinforced with different concentrations (0.10, 0.25, 0.50, and 0.75) of silanated TiO<sub>2</sub> NPs. The resulting nanocomposite materials were characterized in terms of degree of conversion (DC), and sorption/solubility flexural strength, impact strength, Vickers hardness and Martens hardness and compared with unmodified resin and conventional heat-cured (HC) material. The nanocomposites were reassessed after subjecting them to ageing in artificial saliva. A fractured surface was studied under a scanning electron microscope (SEM).

**Results:** The addition of TiO<sub>2</sub> NPs into 3D-printed resin significantly improved flexural strength/modulus, impact strength, Vickers hardness, and DC, while also slightly enhancing Martens hardness compared to the unmodified resin. Sorption values did not show any improvements, while solubility was reduced significantly. The addition of 0.10 wt% NPs provided the highest performance amongst the other concentrations, and 0.75 wt% NPs showed the lowest. Although ageing degraded the materials' performance to a certain extent, the trends remained the same. SEM images showed a homogenous distribution of the NPs at lower concentrations (0.10 and 0.25 wt%) but revealed agglomeration of the NPs with the higher concentrations (0.50 and 0.75 wt%).

**Significance:** The outcomes of this study suggested that the incorporation of TiO<sub>2</sub> NPs (0.10 wt%) into 3D-printed denture base material showed superior performance compared to the unmodified 3D-printed resin even after ageing in artificial saliva. The nanocomposite has the potential to extend service life of denture bases in future clinical use.

## 1. Introduction

Advances in medical technology and expertise has increased human life expectancy [1], leading to a rise in the prevalence of complete edentulism, which is a significant oral health issue among the elderly [2, 3]. Although various treatment options are available, complete removable dentures remain the preferred choice [4,5]. However, the materials used to fabricate dentures must meet specific requirements, including sufficient strength to comply with the minimum acceptable clinical ISO guidelines [6]. Polymethyl methacrylate (PMMA) is the most commonly

used denture base material due to its low cost, excellent aesthetics, outstanding stability, biocompatibility, and ease of repair [7]. However, PMMA has several drawbacks, including low strength, polymerization shrinkage, high susceptibility to microbial colonization and low wear resistance in an aqueous environment [8,9]. To address these issues, researchers have tried various methods to strengthen PMMA, with the use of nanoparticles (NPs) being one of the most promising approaches [10,11]. In dentistry, incorporating nanosized fillers in PMMA has been explored as a means of enhancing properties of these dental materials [12]. The resulting composite material's properties are influenced by the

\* Corresponding author at: Division of Dentistry, School of Medical Sciences, University of Manchester, Manchester M13 9PL, United Kingdom.

\*\* Correspondence to: Dentistry; School of Medical Sciences, University of Manchester, Coupland Building 3, Oxford Road, Manchester M13 9PL, United Kingdom.

E-mail addresses: [atarazi@taibahu.edu.sa](mailto:atarazi@taibahu.edu.sa) (A. Altarazi), [Nikolaos.silikas@manchester.ac.uk](mailto:Nikolaos.silikas@manchester.ac.uk) (N. Silikas).

type, size, shape and concentration of the additional NPs used in conjunction with the type of polymer matrix [13]. One such nanoparticle is  $\text{TiO}_2$ , which is known for its distinct characteristics, including biocompatibility, chemical stability, non-toxicity, corrosion resistance, and high strength and refractive index. Additionally,  $\text{TiO}_2$  NPs have been shown to possess excellent antimicrobial properties [14–17]. Even the smallest addition of  $\text{TiO}_2$  NPs such as 0.5 wt% as a reinforcing agent to a polymeric material can significantly affect the resulting hybrid material's mechanical, physical, optical, and chemical properties [18, 19].

In recent years, digital manufacturing technologies have been widely adopted in dentistry. Computer-aided design and computer-aided manufacturing (CAD-CAM), encompassing subtractive and additive methods, such as 3D-printing and rapid prototyping, have enabled the production of removable dentures [20,21]. 3D-printing is a manufacturing technique that builds products one layer at a time [20, 21]. It has gained popularity in recent years due to the many advantages it offers over the traditional approaches for instance this technology reduces the time a dentist needs to create and fit dentures to just 2–3 sessions. It simplifies the process of making replacements by utilizing previously stored digital data and also eases the burden on dental technicians. Moreover, it either matches or outperforms the traditional method in terms of the overall accuracy of the produced dentures [22–24]. Its fast-evolving nature and wide range of applications makes it an enabling technology in emerging dentistry [20,21].

The use of 3D-printing in creating complete removable denture bases has become increasingly popular both in research and clinical practices. However, this method still has limitations related to its mechanical and physical properties [25,26]. Studies have shown that double bond conversion in 3D printing is poorer than in traditional acrylic resins [25]. Additionally, 3D-printed resin exhibits inferior flexural strength, elastic modulus, impact strength, and surface hardness when compared to the heat-polymerized resin [27,28]. Nevertheless, research has demonstrated that incorporating various additives can enhance the properties of 3D-printed materials. Aati et al. found that adding  $\text{ZrO}_2$  to 3D-printed resin improved the quality of the temporary restoration over time [29]. Similarly, Mubarak et al. found that adding 1 wt% silver-titanium dioxide nanofiller improved the tensile and flexural strength of the 3D-printed material [30]. Chen et al. also demonstrated that the addition of cellulose nanocrystals and silver NPs to a 3D-printed resin improved its flexural and impact strength [31]. Finally, a recent study investigating the effects of  $\text{SiO}_2$  NPs on 3D-printed denture base resin found improvements in impact strength, flexural strength, and hardness [32]. Considering these findings, the addition of NPs appears to be a promising reinforcing strategy for 3D-printable materials.

It seems that previous studies have neither investigated the effect of incorporating  $\text{TiO}_2$  NPs on the mechanical, physical, surface properties, and the degree of conversion (DC) of 3D-printed resins for denture-base fabrication, nor have they examined the impact of aging on the resulting composite material's physio-mechanical properties. Thus, the aims of this study were to assess i) the flexural strength, ii) flexural modulus, iii) impact strength, iv) surface hardness (including Vickers and Martens hardness), v) DC, and vi) sorption and solubility of a series of 3D-printed denture-base resins containing increasing amounts of  $\text{TiO}_2$  NPs after setting and after storage. The null hypotheses were that [1] adding  $\text{TiO}_2$  NPs to the 3D-printed denture base material would have no influence on the properties of 3D-printed denture base resin, and [2] the aging process in artificial saliva would not show any effect on the physical and mechanical properties.

## 2. Materials and methods

### 2.1. Resin and filler materials

The denture bases examined were manufactured using a commercial NextDent denture 3D+ light-cured resin (3D systems, Soesterberg,

Netherlands) in a light pink hue (LOT: WW251N04). The manufacturer indicated that it has an ultimate flexural strength of 84 MPa, a flexural modulus of 2382 MPa, a sorption of  $28 \mu\text{g}/\text{mm}^3$ , and a solubility of  $0.1 \text{ g}/\text{mm}^3$ . The safety data sheet for the product shows that the resin contains Ethoxylated bisphenol A dimethacrylate (75%), 7,7,9-trimethyl-4,13,14-dioxo-3,14-diazahexadecane-1,16-diyl bismethacrylate (10–20%), 2-hydroxyethyl methacrylate (5–10%), Silicon dioxide (5–10%), diphenyl (2,4,6-trimethylbenzoyl) phosphine oxide (1–5%), and titanium dioxide (<0.1%).

Silane (KH-550) coated titanium dioxide NPs in the rutile form (LOT: 7920–111419) with a size of 10–30 nm (99.5%) was bought and added (Skyspring nanomaterials, Texas, USA).

### 2.2. Fabrication and ageing of the specimens

$\text{TiO}_2$  powder was weighed using an electronic scale with a precision of 0.01 mg, and the compositions are shown in Table 1. To ensure a uniform mixture without any powder particle agglomeration, the  $\text{TiO}_2$  powder was progressively added to the liquid resin before being mixed with a speed mixer at 2000 rpm for five min. Due to the higher concentration of NPs, the 0.50 wt% and 0.75 wt% groups required two mixing stages: first, half the amount of powder was mixed with the liquid resin and then the other half was added. The composite material was then poured into the tray of the 3D printer to initiate the printing process.

A total of 420 specimens were manufactured including 3D-printed and HC materials (Fig. 1). A Formlabs Form 2 printer (Formlabs, Somerville, USA), utilising SLA technology with a 405 nm laser wavelength and a  $50 \mu\text{m}$  layer thickness, was used to manufacture 3D-printed specimens in a vertical orientation, which was previously shown to optimise mechanical properties [33]. Preform software (Formlabs, Somerville, USA) was used to prepare the digital specimens before the printing process (Fig. 2). After printing, all specimens were immersed in 99.8% ethanol for five minutes in a Form Wash container (Formlabs, Somerville, USA). After that, specimens were exposed to air for ten minutes to eliminate any residual ethanol traces according to the manufacturer's instructions. Subsequently, the specimens were cured in an ultraviolet (UV) light curing box with a 405 nm LED wavelength and 39 W power at  $60^\circ\text{C}$  (Formlabs, Somerville, USA). The cured specimens were ground using a water lubricant, polished with silicon carbide papers with grain sizes of 400 (P600), 600 (P1200), and 1200 (P2500), and finally polished with  $0.05 \mu\text{m}$  MasterPrep Alumina discs. Fig. 3 represents a schematic stepwise fabrication for the 3D-printed specimens.

In line with the manufacturer's guidelines, the heat-cured material (HC) powder was blended into the liquid until a uniform mixture exhibiting a pliable, dough-like texture was achieved. This blend was then hand-loaded into a mould. Upon sealing the mould and placing it in a hydraulic press exerting a pressure of 15 MPa, surplus material was scraped off from the mould periphery. The mould was subsequently submerged in a curing bath for a span of six h to initiate polymerisation at a temperature of  $80^\circ\text{C}$ . It was then taken out and permitted to gradually cool down for 30 min to ambient temperature prior to unsealing the mould to extract the specimens. A polishing machine (Interlab, Hull, UK) was thereafter utilised to trim, grind, and buff the specimens, employing pumice powder, emery paper and a tungsten carbide bur.

The artificial saliva solution was prepared by dissolving the specific ingredients listed in Table 2 in 1000 ml of distilled water with a pH of 5.52. After being stored in artificial saliva for three months at  $37^\circ\text{C}$ , the specimens were evaluated for mechanical properties. A new solution was added every 14 days to maintain the solution's freshness.

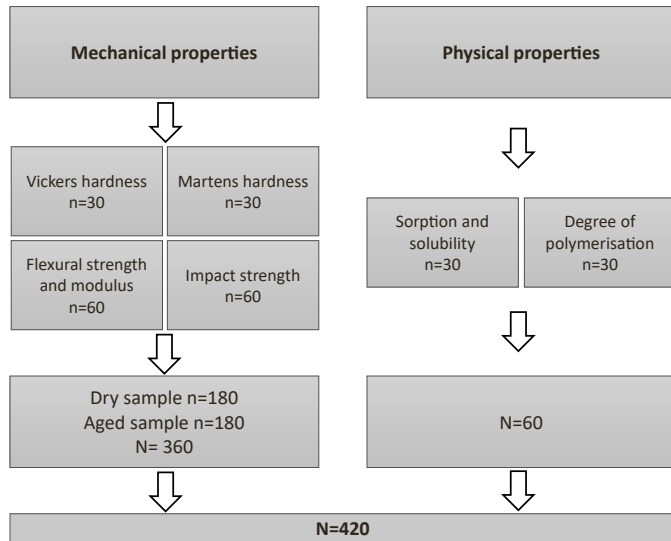
### 2.3. Characterisation of the specimens

#### 2.3.1. FTIR study

Spectra were collected in the  $4000\text{--}400 \text{ cm}^{-1}$  wavelength range at a

**Table 1**Weight percent of TiO<sub>2</sub> in combination with 3D acrylic resin content of the specimen groups.

Groups	Composite material (3D printed liquid resin + TiO <sub>2</sub> )	3D printed liquid resin (g)	Added TiO <sub>2</sub> NPs (g)
A (control)	0%	100.0	0.0
B	0.1 wt%	99.9	0.10
C	0.25 wt%	99.75	0.25
D	0.5 wt%	99.50	0.50
E	0.75 wt%	99.25	0.75

**Fig. 1.** Overall plan for characterisation study.**Fig. 2.** Preparing the digital specimens via Preform software before printing.

resolution of 4 cm<sup>-1</sup>, with an average of 32 scans measured using the Spotlight 200i FT-IR Microscope System at a temperature of 23 ± 1 °C (Fig. A1). To calibrate the equipment, a background spectrum was used.

To determine the DC of the 3D-printed specimens (n = 5), Fourier Transform Infrared (FTIR) spectroscopy was utilized with a single reflection ATR accessory. The resin substance used in 3D printing was scanned once while still in liquid form to provide a baseline record and once again after the final polymerization (15 × 2 disc-shaped specimens). The DC for the 3D-printed material in percentage was determined by evaluating the ratio of the double carbon bond peaks at two frequencies: the stretch of the aliphatic frequency at 1637 cm<sup>-1</sup> against the reference aromatic frequency at 1608 cm<sup>-1</sup> (Eq. 1). For the HC specimens, the referenced peak used was the ester group (C=O) at 1720 cm<sup>-1</sup> (Eq. 2). Regarding the preparation to prevent the oxygen

noise effect, it was self-resolved with the liquid resin form as it covers the crystal properly. The peaks produced appeared with no air noises.

$$DC(\%) = \left( 1 - \frac{\left( \frac{1637^{-1}}{1608^{-1}} \right) \text{ peak heights after polymerisation}}{\left( \frac{1637^{-1}}{1608^{-1}} \right) \text{ peak heights before polymerisation}} \right) \times 100 \quad (1)$$

$$DC(\%) = \left( 1 - \frac{\left( \frac{1637^{-1}}{1720^{-1}} \right) \text{ peak heights after polymerisation}}{\left( \frac{1637^{-1}}{1720^{-1}} \right) \text{ peak heights before polymerisation}} \right) \times 100 \quad (2)$$

### 2.3.2. Sorption and solubility

To conduct sorption and solubility tests per the ISO 20795-1:2013 standard for Denture Base Polymers, each test group (n = 5) with a disc dimensions of 50 × 1 mm underwent the following procedures. First, the specimens were conditioned to room temperature in a desiccator with newly dried silica gel for 60 min before being weighed to acquire the baseline mass (m<sub>1</sub>). The baseline mass was established by daily repeated weighing until the variation between consecutive measurements was no higher than 0.2 mg. Then, the diameter and thickness of each specimen were measured using a digital calliper to determine its volume.

Following that, the specimens were submerged in artificial saliva at 37 ± 2 °C, and their mass was measured daily after each withdrawal from the solution and subsequent drying until the difference between subsequent weighing was no higher than 0.2 mg (m<sub>2</sub>). The specimens were then reconditioned by placing them in a desiccator with freshly dried silica gel for a day at 37 ± 2 °C, followed by another desiccator for an hour at ambient temperature with freshly dried silica gel. The desorption technique was repeated daily until a constant refurbished mass (m<sub>3</sub>) was acquired, with the discrepancy between subsequent weighing was no larger than 0.2 mg.

Using Eqs. (3) and (4), the sorption and solubility in g/mm<sup>3</sup> were calculated. The percentage of mass change and mass loss throughout the sorption and solubility tests were determined using Eq. [5].

$$\text{Sorption} = \frac{m_2 - m_1}{V} \quad (3)$$

$$\text{Solubility} = \frac{m_1 - m_3}{V} \quad (4)$$

$$\text{Change in mass during sorption, SP}(\%) = \left( \frac{m^t - m_1}{m_1} \right) \times 100 \quad (5)$$

Where m<sup>t</sup> is the mass of the specimen at a certain time point.

### 2.3.3. Vickers and martens hardness

A Vickers micro-hardness instrument (FM-700, Future Tech Corp, Tokyo, Japan) was utilised to determine the HV of the specimens. A test load of 50 g was set with a dwell time of 30 s, and each disc (n = 5) with a dimension of 15 × 2 mm was polished as described in Section 2.2 before creating three indentations along a straight line at evenly spaced spots.



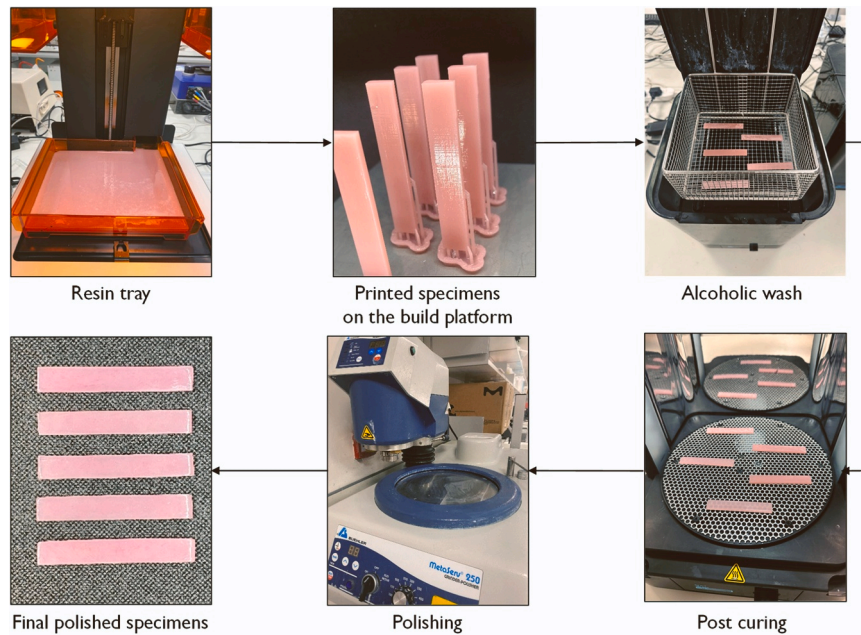


Fig. 3. 3D-printed specimens' stepwise fabrication.

**Table 2**  
Composition of artificial saliva.

Compound	Amount (g/l)	Manufacturer
Sodium chloride (NaCl)	0.400	Acros Organics
Puttasium chloride (KCl)	0.400	Fisher Chemical
Calcium chloride (CaCl <sub>2</sub> )	0.795	Acros Organics
Sodium dihydrogen phosphate (H <sub>2</sub> NaO <sub>4</sub> P)	0.690	Alfa Aesa
Sodium sulfate hydrate (Na <sub>2</sub> SO <sub>4</sub> H <sub>2</sub> O)	0.005	Acros Organics

A Martens Hardness Instrument (Z2.5, ZwickRoell Ltd., Leominster, UK) with a Vickers hardness measurement tip was utilised to determine Martens hardness. The specimen's top surface and the hardness measuring head were kept at a fixed distance of 18 mm at the start of each test session. A force of 50 N was applied at a rate of 5 N/s for 30 s before release. Before contact, the indenter tip was moving at 40 mm/min with an initial approaching rate of 100 mm/min. The proximity between each specimen and the sensor tip was 40 µm. Five controlled indentations were made at baseline with identical spacing on each specimen ( $n = 5$  for each ageing condition). The test load and indentation depth were automatically recorded during the loading and unloading the Vickers indentation tip (136°) and presented as load-displacement curves. To avoid obtaining duplicate measurements at the same location, the indentations were placed along several lines marked on the surface of each specimen. The software (TestXpert®, Zwick GmbH & Co, Ulm, Germany) automatically extracted Martens hardness (HM) as well as other parameters including indentation modulus ( $E_{IT}$ ) and indentation creep ( $C_{IT}$ ). The calculations of HM was based on Eq. [6] from ISO 14577-4/2016.

$$HM = \frac{F}{As(h)} = \frac{F}{26.43 * h^2} \quad (6)$$

HM was expressed in N/mm<sup>2</sup>, where F is the load in N, As (h) is the indenter's surface area at a distance of h from the tip in mm<sup>2</sup>, and As is the indenter's surface area in mm<sup>2</sup> (0.3). Each specimen underwent five indentations 24 h after dry manufacture and again after being stored in artificial saliva for three months.

#### 2.3.4. Flexural strength and modulus

The flexural strength of the specimens was determined through a

three-point bending test conducted on a universal testing machine (Zwick/Roell Z020, Leominster, UK) equipped with a 500 N load cell, following ISO 20795-1:2013 standards for denture base polymers. Specimens ( $n = 10$  with  $64 \times 10 \times 3.3$ ), were first immersed in distilled water at 37 °C for 50 h to establish baseline values. The specimens were then positioned onto a supporting jig, with a distance of  $50 \pm 0.1$  mm between the supports. These were polished cylinders: 3.2 mm in diameter and 10.5 mm in length. The tests were carried out at a preload and test speed of 5 mm/min. This measurement was considered as a baseline measurement. Another set of specimens were kept in artificial saliva for 3 months, and then tested to measure the effect of ageing on the flexural strength and modulus.

Flexural strength was determined using Eq. [7], where F is the maximum applied force in N, l is the distance between the supports in mm, b is the specimen's width in mm, and h is the specimen height in mm. To calculate the flexural modulus, Eq. [8] was used, where d is the deflection in mm at the load of F<sub>1</sub>, F<sub>1</sub> is the load in N at the point on the straight line (with the highest slope) of the load/deflection curve.

$$\sigma = \frac{3Fl}{2bh^2} \quad (7)$$

$$E = \frac{F_1 l^3}{4bh^3 d} \quad (8)$$

#### 2.3.5. Impact test

The Charpy un-notched impact test was conducted using a universal pendulum impact testing device (Zwick/Roell Z020 Leominster), following EN ISO 179-1:2010 standards ( $n = 10$  for each ageing condition). The specimens, with dimensions of  $80 \text{ mm} \pm 0.5$  in length,  $10 \text{ mm} \pm 0.2$  in width, and  $4 \pm 0.2$  mm in thickness, were horizontally supported at both ends ( $40 \pm 0.2$  mm) and struck at the centre using a free-swinging pendulum with a 4.0 J load cell released from a fixed height. The amount of energy absorbed during impact was recorded in joules (J). The Charpy impact strength ( $a_{CU}$ ) (kJ/m<sup>2</sup>) was calculated using Eq. 9. This measurement was regarded as the baseline reading. A separate collection of specimens were stored in artificial saliva for a duration of 3 months to determine the impact strength of the aged specimens.

$$acU = \frac{Wb}{bh} \times 10^3 \quad (9)$$

Where  $Wb$  represents the energy at break in joules, and  $b$  and  $h$  are the specimen's width and thickness in mm, respectively.

### 2.3.6. SEM and EDX analysis

Specimens were mounted on an aluminium stub, and a thin layer of gold was deposited before placing it in the scanning electron microscope (SEM) chamber. Images were captured at different magnifications ranging from  $\times 1000$  to  $\times 100,000$  using a secondary electron detector with an acceleration voltage of 10.0 kV.

### 2.4. Statistical analysis

All data were statistically analysed using SPSS version 25 (IBM, New York, NY, USA). The Shapiro-Wilk test was used to determine the distribution of the data, and the Levene test was utilized to confirm its homogeneity. The data were statistically analysed using one-way ANOVA, followed by Tukey's/Games-Howell post-hoc analysis according to data homogeneity, to compare the means between groups with a significance level set at  $p \leq 0.05$ .

## 3. Results

### 3.1. Fractured surface analysis

SEM images at a magnification of  $\times 100k$  revealed the presence of two types of fillers within the tested 3D-printed specimens. Silicon dioxide ( $SiO_2$ ), as reported by the manufacturer to make up 5–10% by weight, appeared as crystal-shaped rods (Fig. A2), and  $TiO_2$  NPs that were added to the resin material in this study at different weight percentages, and they appeared as smaller spherical clusters. The smaller spherical particles were not found within the unmodified NextDent resin. To further investigate the distribution and quantity of  $TiO_2$  NPs present within the specimens, EDX mapping and analysis were performed. EDX mapping at many sites confirmed the distribution of  $TiO_2$  NPs, showing that as the amount of NP increased, so did their agglomeration (Fig. A3 and Fig. A4). Furthermore, EDX quantitative spectral analysis confirmed the presence of  $TiO_2$  NPs and verified the variation in the amount of NP corresponding to each group (Table A1). On group A, although there were minor traces of  $TiO_2$  NPs ( $<0.1$  wt%), it was not shown on the SEM and EDX analysis, as a minimal amount of the NPs are needed before it to be possible to be detected.

### 3.2. Degree of conversion

Fig. 4 presents the means and standard deviations of DC for the examined materials. Group A exhibited the lowest DC, showing a

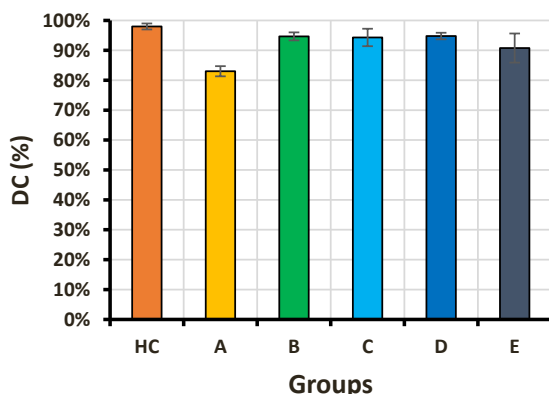


Fig. 4. Mean values of DC of the tested materials.

significant difference in comparison to HC group ( $p < 0.05$ ). For the nanocomposite groups, the DC rose significantly compared to Group A, and the results became not significantly different compared to HC, except for Group E, at which point the value declined and became significantly lower than HC ( $p < 0.05$ ). The remaining  $TiO_2$  NPs groups had lower values compared to HC, but these differences were not statistically significant ( $p > 0.05$ ).

### 3.3. Sorption and solubility

The means and standard deviations for sorption and solubility are provided in Figs. 5 and 6 respectively. The lowest sorption value was observed for the HC group, which was significantly lower than the other groups ( $p < 0.05$ ). This was followed by 3D-printed/ $TiO_2$  NPs groups (except Group E), where they displayed non-significant differences compared to Group A ( $p > 0.05$ ). Group E showed the highest sorption with a significant difference compared to the other groups ( $p < 0.05$ ).

In contrast, solubility exhibited a different pattern. The highest solubility value was associated with the Group A, followed by the HC and they were not significantly different from each other ( $p > 0.05$ ). Both groups had significantly higher solubility values compared to the 3D-printed/ $TiO_2$  NPs groups, with the exception of Group E, which showed the highest solubility amongst the 3D-printed/ $TiO_2$  NPs groups and were not significantly different compared to Group A and HC ( $p > 0.05$ ).

All study groups manifested changes in mass over time when stored in artificial saliva. Throughout the sorption process, there was a rapid mass increase in the initial 14 days, which then slowed until equilibrium was achieved on day 42, as depicted in Fig. 7. Subsequently, during the desorption process, the mass consistently reduced in the first 7 days and then continued to decrease slowly until equilibrium was reached on the 28th day of the desorption process.

### 3.4. Hardness

The mean and standard deviation of Vickers hardness are displayed in Fig. 8. Before aging, no significant difference was observed among the groups except for Group A, which was significantly lower than others ( $p < 0.05$ ). After aging, Group B showed the highest hardness, while HC showed the lowest. HV reduced with increase in  $TiO_2$  NPs to be significantly lower with Groups D and E compared to other 3D-printed/ $TiO_2$  NPs groups ( $p < 0.05$ ). When comparing the same group before and after aging, HV dropped significantly in the HC, E, and D groups ( $p < 0.05$ ). However, this observation was not seen with the other 3D-printed/ $TiO_2$  NPs groups, where the decrease was not significant ( $p > 0.05$ ).

Fig. 9 presents the mean and standard deviation of Martens hardness for all groups before and after aging. Before aging, no statistically significant differences were observed between the groups (column wise).

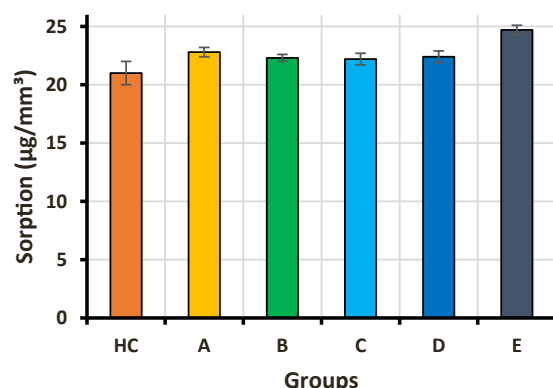


Fig. 5. Sorption values of the tested materials in artificial saliva for six weeks.

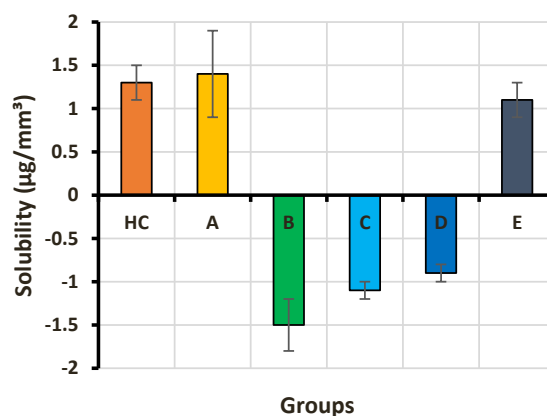


Fig. 6. Solubility values of the tested materials in artificial saliva for five weeks.

On the other hand, the aged HC group exhibited a significantly lower value compared to the other aged groups ( $p < 0.05$ ), except for the Group E ( $p > 0.05$ ). However, when comparing HM between before and after ageing within each group (row wise), all decreased after the ageing process without significant differences, except for the HC group, where MH dropped significantly. The indentation modulus (Table A2) demonstrated a trend similar to that of Martens hardness, with the notable exception of the Group A, which exhibited a significantly lower value before the ageing process compared to other groups. Within each group, the ageing process did not induce any significant impact, except for the Group A, where the result significantly increased. The indentation creep (Table A2) was significantly greater with HC compared to the other groups before ageing, and the ageing process significantly affected only Group D and E.

### 3.5. Flexural strength and modulus

Fig. 10 and Fig. 11 display the means and standard deviations of flexural strength and modulus for the control and tested materials before and after the ageing process. In terms of flexural strength, the HC group registered the lowest value, showing a significant difference compared to the other groups. Conversely, Group B exhibited the highest value with a significant difference compared to the other groups ( $p < 0.05$ ). The flexural strength of the materials decreased as the amount of  $\text{TiO}_2$  NPs increased beyond 0.10 wt% (Group B), with the lowest value associated with group E compared to the other nanocomposite groups. The ageing process significantly and negatively impacted all groups containing  $\text{TiO}_2$  NPs ( $p < 0.05$ ) except for Group C. Although the values for the HC and Group A also decreased after the ageing process, the

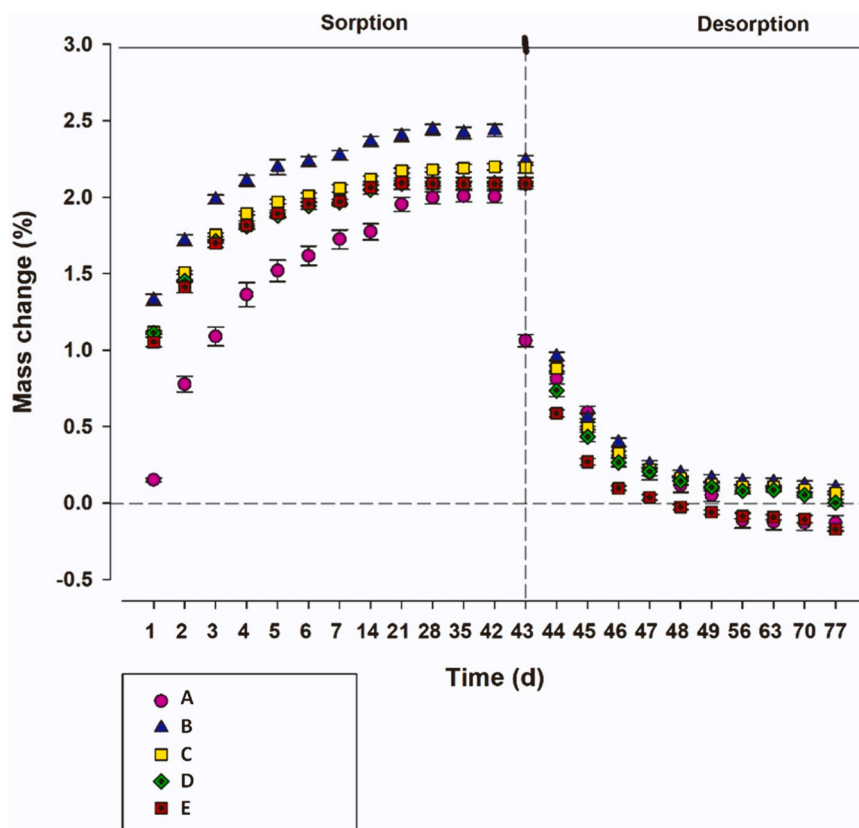


Fig. 7. Mass change of specimens immersed in artificial saliva over 77 days.



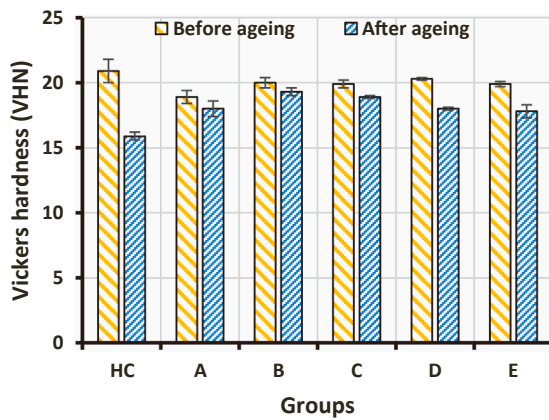


Fig. 8. HV of the tested materials before and after ageing in artificial saliva for three months.

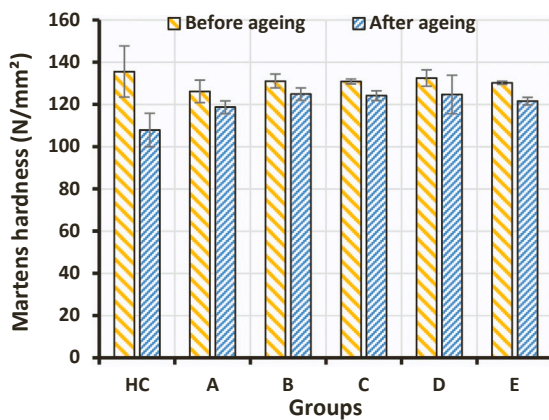


Fig. 9. HM of the three tested materials before and after ageing in artificial saliva for three months.

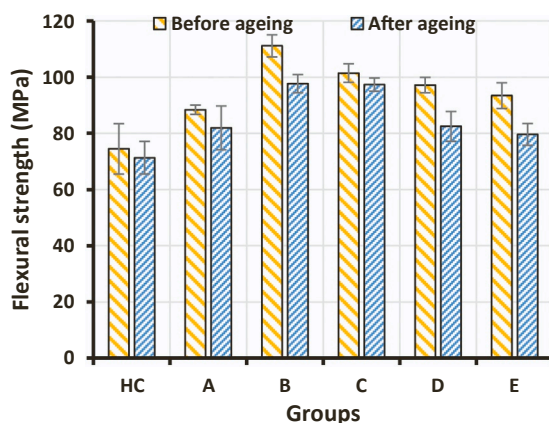


Fig. 10. Flexural strength of the tested materials before and after ageing in artificial saliva for three months.

decline was not significant ( $p > 0.05$ ).

The flexural modulus exhibited a pattern nearly similar to the flexural strength. The HC group had the lowest value, but no significant difference was observed compared to Group A and E ( $p > 0.05$ ). Groups B and C demonstrated the highest value, with a significant difference compared to all other tested groups ( $p < 0.05$ ). The ageing process significantly affected some of the groups containing TiO<sub>2</sub> NPs and the HC group ( $p < 0.05$ ).

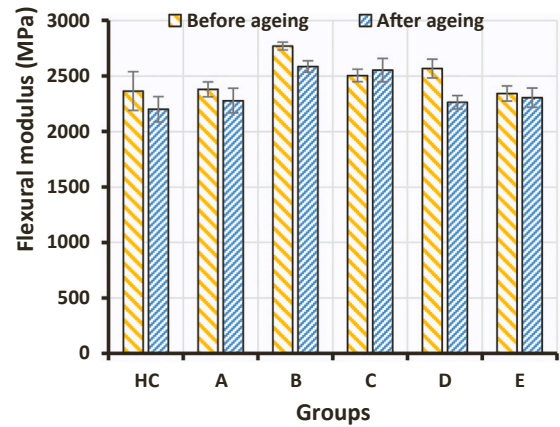


Fig. 11. Flexural modulus of the tested materials before and after ageing in artificial saliva for three months.

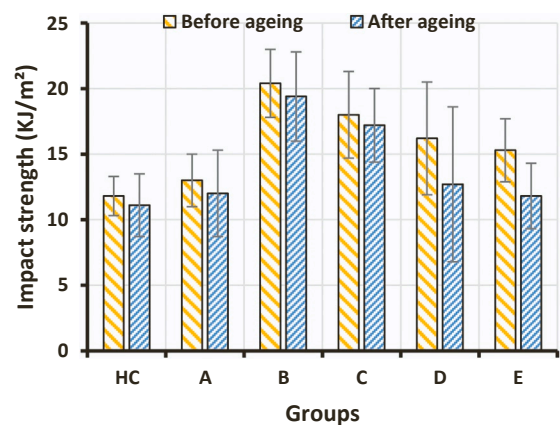


Fig. 12. Impact strength of the tested materials before and after ageing in artificial saliva for three months.

### 3.6. Impact strength

The means and standard deviations of the impact strength are displayed in Fig. 12. Before aging, no statistically significant difference was observed between the HC and Group A ( $p > 0.05$ ). However, a significant difference was noted between these groups and Group B ( $p < 0.05$ ). The impact strength values of Groups D and E decreased slightly compared to Group B, and became not significantly different from the other groups, including Group A and HC ( $p > 0.05$ ).

After aging, the results were similar, except for Group E, which exhibited a significantly lower value compared to Groups B and C ( $p < 0.05$ ). Furthermore, ageing process did not show any significant difference on the impact strength ( $p > 0.05$ ).

## 4. Discussion

The effect of adding TiO<sub>2</sub> NP into a 3D-printed denture base resin was investigated in this study. According to the results, the first null hypothesis was rejected, as the addition of TiO<sub>2</sub> NPs altered the properties of the 3D-printed denture base resin. Furthermore, the second null hypothesis was also rejected, as the ageing process in artificial saliva adversely affected some of the properties of the 3D-printed nanocomposites.

TiO<sub>2</sub> NPs are a preferred additive metal oxide to be added to denture base resin due to their advantages, including cost-effectiveness, ease of availability, biocompatibility, chemical stability, solid physical properties, and antimicrobial properties [34]. Numerous researchers have



incorporated metal oxide NPs into dental resin materials, and treated their surfaces to prevent agglomeration, which arises from the repulsive interaction between PMMA and the NPs [35]. Moreover, achieving a uniform distribution was difficult due to the Van der Waals forces between the NPs, which may further cause agglomeration and hence adversely affect the composite material [36]. The goal was to achieve a homogeneous distribution and interaction of the NPs within the matrix of material. To accomplish this, researchers have altered the surfaces of the NPs with modifiers, such as proteins and acids [32,37–39]. In this study, TiO<sub>2</sub> NPs with silanated surfaces were used in conjunction with a speed mixing technique to minimize agglomeration and achieve as uniform a distribution of the NPs as possible.

The amount of TiO<sub>2</sub> NPs incorporated in this study was based on two factors. First, two previous studies used TiO<sub>2</sub> NPs with 3D-printed denture base resins [40,41], where they used a range of 0.10 – 2.5 wt % TiO<sub>2</sub> NPs. Second, in a pilot run in this study aimed to check the printability of the composite material with difference percentages of TiO<sub>2</sub> NPs. It was found that the addition of 2.0 wt% of TiO<sub>2</sub> NPs increased the viscosity of the liquid resin and led to failure in printing, so a range of TiO<sub>2</sub> NPs between 0.10 and 1.0 wt%. was used After initial experiments, it was found that the properties significantly decreased after adding 0.75 wt% TiO<sub>2</sub> NPs, hence a range between 0.10 and 0.75 wt% TiO<sub>2</sub> NPs was considered for this work.

Flexural strength is a critical property for denture bases, as it is considered the primary mode of clinical failure [39]. The results in this study indicated a higher flexural strength of Group A (89.2 MPa) compared to HC (74.5 MPa), which was opposite to the findings in other studies [32,39,42]. The reason behind this could be related to the HC control material used in other studies with differences in their compositions compared to the HC material used in this study, as well as the printing settings and the chemical composition of the 3D-printed materials used. Lowery et al. [27] reported a value of 90 MPa for their tested material, and Aati et al. recorded 134 MPa when testing the flexural strength of 3D-printed denture base material [43]. All the previous FS recorded revealed a similar or higher flexural strength compared to the current results, which confirm that the various outcomes between 3D-printed and heat-cured materials mainly depend on the materials used in different studies. Also, the printing parameters could have a direct effect on the mechanical properties of the 3D-printed material; for example, one study used a horizontal printing orientation and reported a lower flexural strength of 3D-printed denture base material compared to the conventional material [27], while a different study used a vertical printing orientation, and indicated a higher flexural strength of the 3D-printed material compared to the conventional one [44].

The integration of TiO<sub>2</sub> NPs into 3D-printed resin significantly increased both flexural strength and modulus. Group B exhibited the highest readings in comparison to the Group A and HC. However, the results began to decline as the concentration of NPs increased beyond this point, with group E showing no significant difference compared to Group A. The enhancement in flexural strength and modulus after the addition of TiO<sub>2</sub> NPs is a concentration-dependent process. TiO<sub>2</sub> NPs are physically rigid particles that can fill voids within the material's matrix. With proper distribution, they can absorb energy and stresses before failure. TiO<sub>2</sub> nanoparticles, being physically rigid, can play a significant role in absorbing energy within the material. When external forces or stresses are applied to the material, these nanoparticles can help distribute the stress more evenly throughout the matrix. As a result, they act as stress absorbers, reducing the concentration of stress at specific points. [34,36,45]. Lower concentrations of TiO<sub>2</sub> NPs (Groups B and C) yielded the highest flexural strength and modulus, consistent with other studies involving different types of NPs with 3D-printed dental resins (such as SiO<sub>2</sub>, ZrO<sub>2</sub>, and TiO<sub>2</sub> NPs) [29,32,41]. As the NP concentration increased, properties began to decrease. This was confirmed by previous studies and attributed to NP agglomeration within the matrix that can create stress concentration areas, thus weakening the material's internal

structure [46,47].

The main factor for denture failure after an accidental drop onto a hard surface is the lower impact strength associated with denture base materials [28,48]. Hence, adequate impact strength is required to protect the denture base from this type of failure. Impact strength showed a similar behaviour to flexural strength and modulus, as impact strength of Group A was slightly higher compared to the HC. Group B showed a significantly increased the impact strength compared to the Groups A and HC, and reduced with more addition until Group E, where the IS was slightly higher but not significantly different compared to Group A and HC. Other studies reported the same observation after incorporating different types of NPs into 3D-printed and heat-cured denture base resins [14,17,32,39,49]. The interpretation of this observation is fairly similar to the analysis with the flexural strength and modulus mentioned above.

Group A had lower HV compared to that of the HC, in line with other studies reporting similar observations [28,50]. This could be related to the difference in DC between the materials, as HC had a significantly higher DC compared to Group A. After adding TiO<sub>2</sub> NPs, HV increased significantly, and this increase was directly proportional with the increase in DC. Aati et al. [29] studied the effect of adding ZrO<sub>2</sub> NPs to 3D-printed denture bases and noticed that HV values increased until a certain point, where the composite material became saturated. Similarly, Gad et al. investigated the effect of adding SiO<sub>2</sub> NPs and found a significant increase in HV compared to the unmodified material. Both of the aforementioned studies' findings were agreeing with the findings in this study. It is worthy to mention that although the increase in the HV was statistically significant, the clinical benefit of that increase might be irrelevant.

HM exhibited behaviour similar to the HV. Group A displayed a lower value compared to HC, and as TiO<sub>2</sub> NPs were added, HM increased, which was also correlated to DC for each group. This can be attributed to the enhancement of material stiffness and the reduction of matrix mobility due to the addition of rigid particles that may be present on the surface of the specimen, which decreases the elastic-plastic deformation. Similar observations were found in other studies, indicating an increase in surface hardness for heat-cured denture base materials after adding TiO<sub>2</sub> NPs [17,49,51,52].

To further explain the change in surface hardness, DC for each group was investigated. As shown in Fig. 4, DC of the HC sample was highest. A potential explanation for the enhanced DC of the HC material in comparison to the 3D-printed materials could be the manufacturing process. The HC material is polymerised under more extreme conditions of temperature and pressure, and for a prolonged period (cycled for six hours in a water bath); this could potentially contribute positively to the DC [53–55]. Another possibility is the filler content of the materials, as a higher DC could be attributed to the absence of fillers within the matrix of HC material. The addition of filler particles, such as silicon dioxide found within 3D-printed resin to increase the viscosity of the material, can affect the polymerization process of the resin matrix by reducing the mobility of the unreacted monomers [29]. This may lead to a change in the DC, which is a measure of the extent to which monomers are converted into polymers during the polymerization process [56]. However, the results of this study indicated that the addition of TiO<sub>2</sub> NPs increased the DC of the resultant composite material. In some cases, certain types of fillers with specific shape, size, concentration, and distribution within the resin matrix can increase DC. In this case, TiO<sub>2</sub> NPs might have helped scatter curing light energy within the 3D-printed material and increased the rate of DC, which may explain the increase in surface hardness and the mechanical properties of the composite material compared to the unmodified one [57,58].

Water sorption and solubility of denture base are important properties that can indirectly measure denture durability within the oral cavity. The polar nature of the polymeric material, due to the presence of the ester group, can interact with water molecules through hydrogen bonding, which could lead to water absorption and consequently affect the properties of the material [59,60]. Sorption and solubility tests in

this study were conducted in artificial saliva until equilibrium was reached, at which point the specimen could no longer gain further mass. The sorption process lasted about 2–4 weeks, while the solubility test (desorption) lasted around 1–2 weeks for all groups. Sorption increased in the following order:  $HC < C < B < D < A < E$ . A relationship between sorption and DC can be established here, as HC showed the highest DC, followed by 3D-printed/  $TiO_2$  NPs groups and finally Group A. A higher of DC is an indication of a more densified and cross-linked polymeric matrix, which has fewer unreacted monomers and fewer spaces for water molecules. As a result, the material with a higher DC will typically have lower water sorption [43,61–63]. HC specimens showed the lowest saliva sorption compared to other groups, which might be related to the higher DC that resulted from a long polymerization cycle (6 h in a water bath) to achieve full polymerization and the lowest amount of void formation [54]. With the addition of  $TiO_2$  NPs, DC was enhanced compared to the unmodified resin as explained earlier. Additionally, the addition of  $TiO_2$  NPs could fill the pores within the material, decreasing the uptake of water molecules. The type of silane used is KH-550, which is characterized by having an epoxy (oxirane) functional group, a methoxy group, and a propyl chain attached to the silicon atom. The epoxy group is reactive and can form chemical bonds with a variety of dental resins. This makes KH-550 suitable for promoting adhesion between polymers and inorganic surfaces by facilitating covalent bonding between the two. Furthermore, the hydrophobic nature of silane coated  $TiO_2$  NPs could aid in decreasing the water uptake [17]. Group E had the highest sorption value compared to other 3D-printed/  $TiO_2$  NPs groups, and the lowest DC, which may have resulted from the agglomeration of particles that adversely affected various properties of the material. The observation in this study was in agreement with a study that used  $ZrO_2$  NPs with 3D-printed provisional dental restorations [29], and other studies which investigated the addition of  $TiO_2$  NPs to heat-cured denture base materials [17,64]. But saliva solubility showed different behaviour. Solubility depends mainly on the leached-out materials such as unreacted monomers, plasticizers, and initiators [65]. The addition of  $TiO_2$  NPs decreased solubility significantly, and the solubilities from lowest to highest were as follows:  $B < C < D < E < HC < A$ . Two possible explanations can be drawn for this observation: [1] the increased DC with the 3D-printed/  $TiO_2$  NPs groups, which decreases the amount of unreacted monomers, and [2] the interaction between  $TiO_2$  NPs and saturated remaining monomers [53].

Clinically, denture bases are exposed to repeated processes of sorption/desorption. Along with the dynamic intraoral environment, both apply significant stresses to the brittle nature of the prosthesis, which can greatly affect its properties. The aim of our aging assessment of the materials in artificial saliva was to mimic the oral environment and then evaluate the effect of aging on the material properties. In general, the aging process in artificial saliva adversely affected all the mechanical and surface properties of the materials, with some differences among the groups. For example, HV and HM of the HC group were significantly affected by the aging process, while only HV of Groups E and D were significantly affected, which showed that the elastic/plastic behaviour of the 3D-printed material acted differently. This could be explained by the different composition of the two materials, and as the composition of the 3D-printed material was not clearly illustrated by the manufacturer, a definite conclusion cannot be reached on that. But flexural strength and impact strength of the HC samples and the Group A were not affected significantly by the aging process. However, the 3D-printed/

$TiO_2$  NPs groups showed a significant reduction in the properties, especially with higher concentrations of  $TiO_2$  NPs, where the concentration of the NPs at higher levels can agglomerate within the material and act as local stress areas where cracks can initiate and negatively affect the properties of the material. SEM images approved the presence of agglomeration within the groups with higher concentrations of  $TiO_2$  NPs.

3D-printed materials hold promise as an alternative to traditional materials, a notion supported by the findings of this study. Nevertheless, it is important to approach the results published in this field with caution. The wide array of conclusions observed in the literature may arise from various factors, including variations in resin composition, printing orientations, and post-printing polymerization processes, all of which can impact the quality of the produced objects. One of the limitations of this study is its reliance on a single type of heat-cured material. Additionally, it is worth noting that the specimen dimensions used in the study did not replicate those of a real denture base, which could be done in a future work to acquire more reliable results.

The results of all the properties for all groups were compatible with the ISO recommendations, even after applying the artificial ageing process to the materials. Further studies on colour stability and accuracy are suggested, as the  $TiO_2$  NPs are whitish in colour, and the change in colour with higher concentrations is very noticeable (Fig. A5). Additionally, exploring biological properties is worthwhile, since  $TiO_2$  NPs have antibacterial capabilities which could benefit denture wearers by protecting against bacterial/fungal growth.

#### 4.1. Clinical significance

Clinically, 3D-printed denture base material has proven to be a promising alternative to conventional heat-cured materials. Combining this with nanotechnology could further improve the current denture properties leading longer service life and patient satisfaction and address the drawbacks of existing conventional materials.

## 5. Conclusions

- (1) Incorporating  $TiO_2$  NPs into 3D-printed NextDent denture base resin significantly increased the properties such as flexural strength/modulus and impact strength, Vickers hardness, as well as DC and solubility compared to the unmodified material. The best outcomes were associated with the addition of 0.1 wt%  $TiO_2$  NPs. However, the effect on saliva sorption and Martens hardness, was not significant.
- (2) An increased concentration of  $TiO_2$  NPs of 0.5 wt% and higher showed agglomeration of the NPs under the microscope, which lowered the material properties compared to those with lower concentrations of  $TiO_2$  NPs.
- (3) The aging process in artificial saliva negatively affected both the heat-cured and modified 3D-printed materials, particularly with respect to flexural strength, where the effect was significant.

## Acknowledgment

The authors thank the Researchers Supporting Project (RSPD2023R790), King Saud University, Riyadh, Saudi Arabia.

## Appendix

**Table A1**

Mean and standard deviation (SD) of DC, sorption, and solubility for the control and the test groups.

Groups	DC (%)	Sorption ( $\mu\text{g}/\text{mm}^3$ )	Solubility ( $\mu\text{g}/\text{mm}^3$ )
HC	98.0 (1.0) <sup>A</sup>	21.0 (1.0) <sup>A</sup>	1.3 (0.2) <sup>A</sup>
A	84.0 (1.7) <sup>B</sup>	22.8 (0.4) <sup>B</sup>	1.4 (0.4) <sup>A</sup>
B	94.7 (1.3) <sup>AC</sup>	22.3 (0.3) <sup>B</sup>	-1.5 (0.3) <sup>B</sup>
C	94.3 (2.9) <sup>AC</sup>	22.2 (0.5) <sup>B</sup>	-1.1 (0.1) <sup>BC</sup>
D	94.8 (1.1) <sup>AC</sup>	22.4 (0.5) <sup>B</sup>	-0.9 (0.1) <sup>C</sup>
E	90.8 (4.9) <sup>C</sup>	24.7 (0.4) <sup>C</sup>	1.1 (0.2) <sup>A</sup>

\*Within a column, cells having similar letters are not significantly different from the control (HC), and within a row, cells having similar numbers are not significantly different (before and after ageing for the same material).

**Table A2**

Mean and standard deviation (SD) of Martens hardness for the control and the test groups before and after ageing process in artificial saliva.

Groups	Martens hardness (N/mm <sup>2</sup> )		Indentation modulus (kN/mm <sup>2</sup> )		Indentation creep (%)		Vickers hardness (VHN)	
	Before ageing	After ageing	Before ageing	After ageing	Before ageing	After ageing	Before ageing	After ageing
HC	135.6 (12.1) <sup>A,1*</sup>	107.9 (7.9) <sup>A,2</sup>	3.3 (0.3) <sup>A,1</sup>	2.8 (0.4) <sup>A,1</sup>	12.0 (0.9) <sup>A,1</sup>	11.6 (0.2) <sup>A,1</sup>	20.9 (0.9) <sup>A,1*</sup>	15.9 (0.3) <sup>A,2</sup>
A	126.2 (5.3) <sup>A,1</sup>	118.7 (3.0) <sup>AB,1</sup>	2.3 (0.2) <sup>B,1</sup>	3.0 (0.3) <sup>A,2</sup>	6.8 (0.1) <sup>B,1</sup>	6.7 (0.2) <sup>B,1</sup>	18.9 (0.5) <sup>B,1</sup>	18.0 (0.6) <sup>BC,1</sup>
B	131.1 (3.3) <sup>A,1</sup>	124.9 (2.9) <sup>B,1</sup>	2.9 (0.1) <sup>A,1</sup>	3.0 (0.2) <sup>A,1</sup>	7.4 (0.1) <sup>B,1</sup>	6.9 (0.1) <sup>B,1</sup>	20.0 (0.4) <sup>A,1</sup>	19.3 (0.3) <sup>B,1</sup>
C	130.9 (1.2) <sup>A,1</sup>	124.2 (2.3) <sup>B,1</sup>	2.8 (0.1) <sup>A,1</sup>	2.8 (0.1) <sup>A,1</sup>	7.4 (0.3) <sup>B,1</sup>	7.4 (0.1) <sup>B,1</sup>	19.9 (0.3) <sup>A,1</sup>	18.9 (0.1) <sup>BC,1</sup>
D	132.5 (3.9) <sup>A,1</sup>	124.8 (9.1) <sup>B,1</sup>	2.9 (0.2) <sup>A,1</sup>	2.9 (0.4) <sup>A,1</sup>	7.0 (0.1) <sup>B,1</sup>	8.6 (0.5) <sup>C,2</sup>	20.3 (0.1) <sup>A,1</sup>	18.0 (0.1) <sup>C,2</sup>
E	130.3 (0.8) <sup>A,1</sup>	121.6 (1.8) <sup>AB,1</sup>	2.9 (0.04) <sup>A,1</sup>	2.7 (0.2) <sup>A,1</sup>	7.3 (0.1) <sup>B,1</sup>	8.5 (0.1) <sup>C,2</sup>	19.9 (0.2) <sup>A,1</sup>	17.8 (0.5) <sup>C,2</sup>

\*Within a column, cells having similar letters are not significantly different from the control (HC), and within a row, cells having similar numbers are not significantly different (before and after ageing for the same material).

**Table A3**

Mean and standard deviation (SD) of flexural strength and modulus for the control and the test groups before and after ageing process in artificial saliva.

Groups	Flexural strength (MPa)		Flexural modulus (MPa)		Impact strength (KJ/m <sup>2</sup> )	
	Before ageing	After ageing	Before ageing	After ageing	Before ageing	After ageing
HC	74.5 (8.5) <sup>A,1*</sup>	71.2 (6.1) <sup>A,1</sup>	2377.6 (122.4) <sup>A,1*</sup>	2181.1 (31.1) <sup>A,2</sup>	11.8 (1.5) <sup>A,1*</sup>	11.1 (2.4) <sup>A,1</sup>
A	89.2 (1.7) <sup>B,1</sup>	82.0 (7.8) <sup>B,1</sup>	2391.4 (70.1) <sup>A,1</sup>	2278.6 (111.0) <sup>A,1</sup>	13.0 (2.0) <sup>AC,1</sup>	12 (3.3) <sup>AC,1</sup>
B	111.2 (4.0) <sup>C,1</sup>	97.7 (3.2) <sup>C,2</sup>	2769.6 (35.0) <sup>B,1</sup>	2586.0 (51.4) <sup>B,2</sup>	20.4 (2.6) <sup>B,1</sup>	19.4 (3.4) <sup>B,1</sup>
C	101.5 (3.3) <sup>D,1</sup>	97.3 (2.4) <sup>C,1</sup>	2575.3 (58.6) <sup>C,1</sup>	2554.1 (105.7) <sup>B,1</sup>	18.0 (3.3) <sup>BC,1</sup>	17.2 (2.8) <sup>BCD,1</sup>
D	97.2 (2.8) <sup>DE,1</sup>	82.5 (5.3) <sup>B,2</sup>	2567.7 (84.5) <sup>C,1</sup>	2263.8 (60.3) <sup>A,2</sup>	16.2 (4.3) <sup>AB,1</sup>	12.7 (5.9) <sup>AD,1</sup>
E	93.4 (4.6) <sup>BE,1</sup>	79.6 (3.9) <sup>B,2</sup>	2342.5 (68.2) <sup>A,1</sup>	2305.1 (86.4) <sup>A,1</sup>	15.3 (2.4) <sup>AB,1</sup>	11.8 (2.5) <sup>A,1</sup>

\*Within a column, cells having similar letters are not significantly different from the control (HC), and within a row, cells having similar numbers are not significantly different (before and after ageing for the same material).

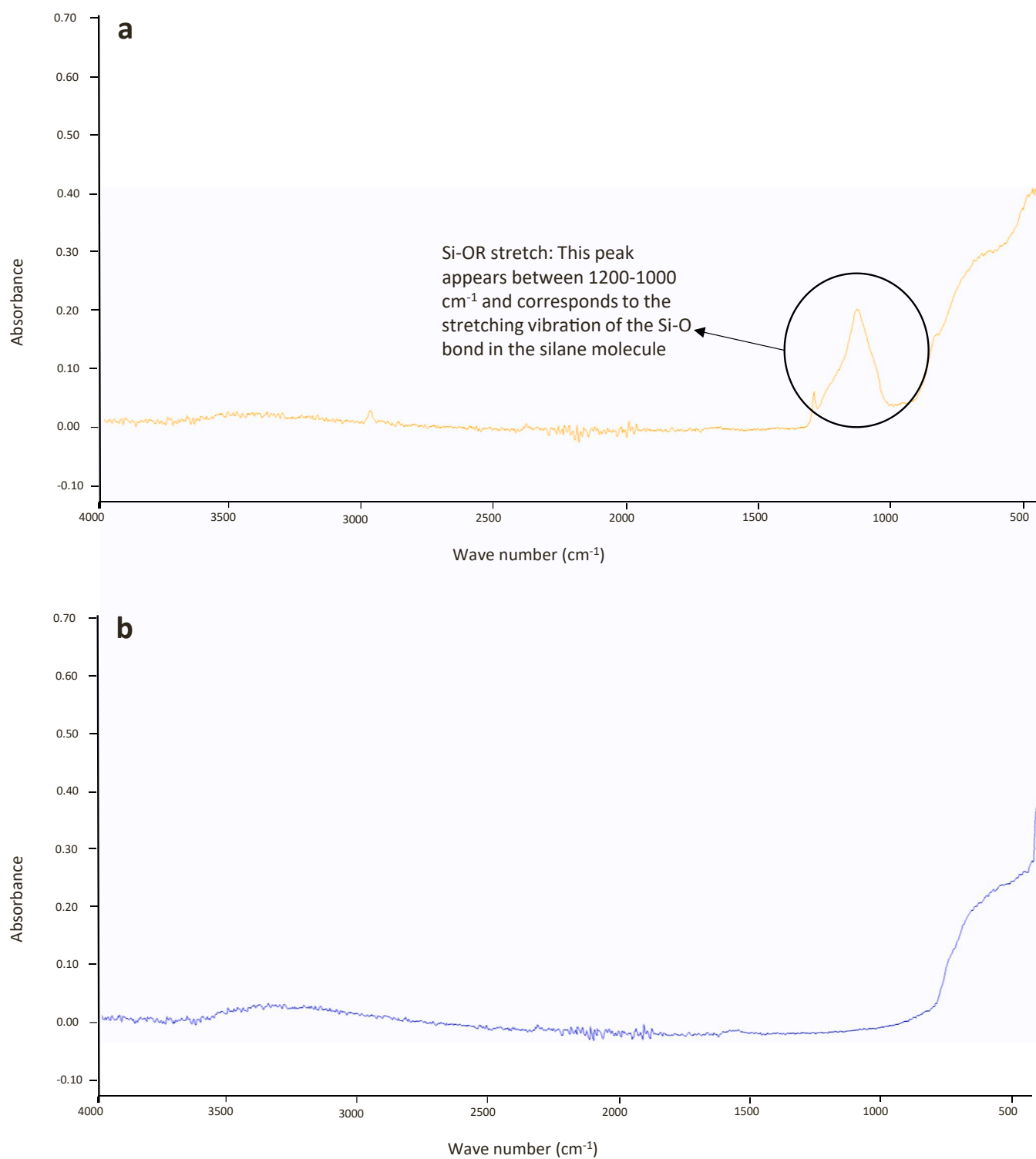


**Fig. A1.** FTIR analysis for: (a) silane coated vs. (b) non-silane coated  $\text{TiO}_2$  NPs.



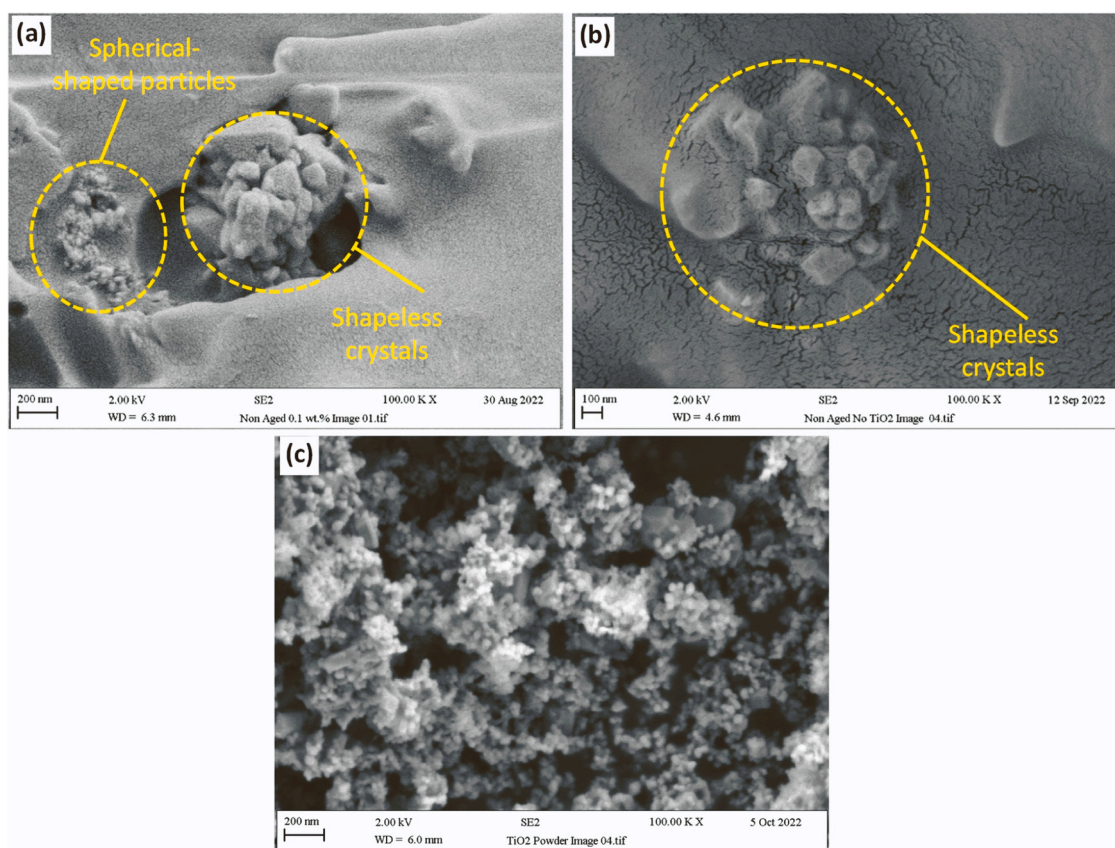


**Fig. A2.** Fractured surface morphology of 3D printed denture base resin materials with a magnification of  $\times 100k$  times showing different types of filler in: (a) 3D-printed  $\text{TiO}_2$  reinforced composite material, (b) unmodified 3D-printed material, (c)  $\text{TiO}_2$  NPs powder only.

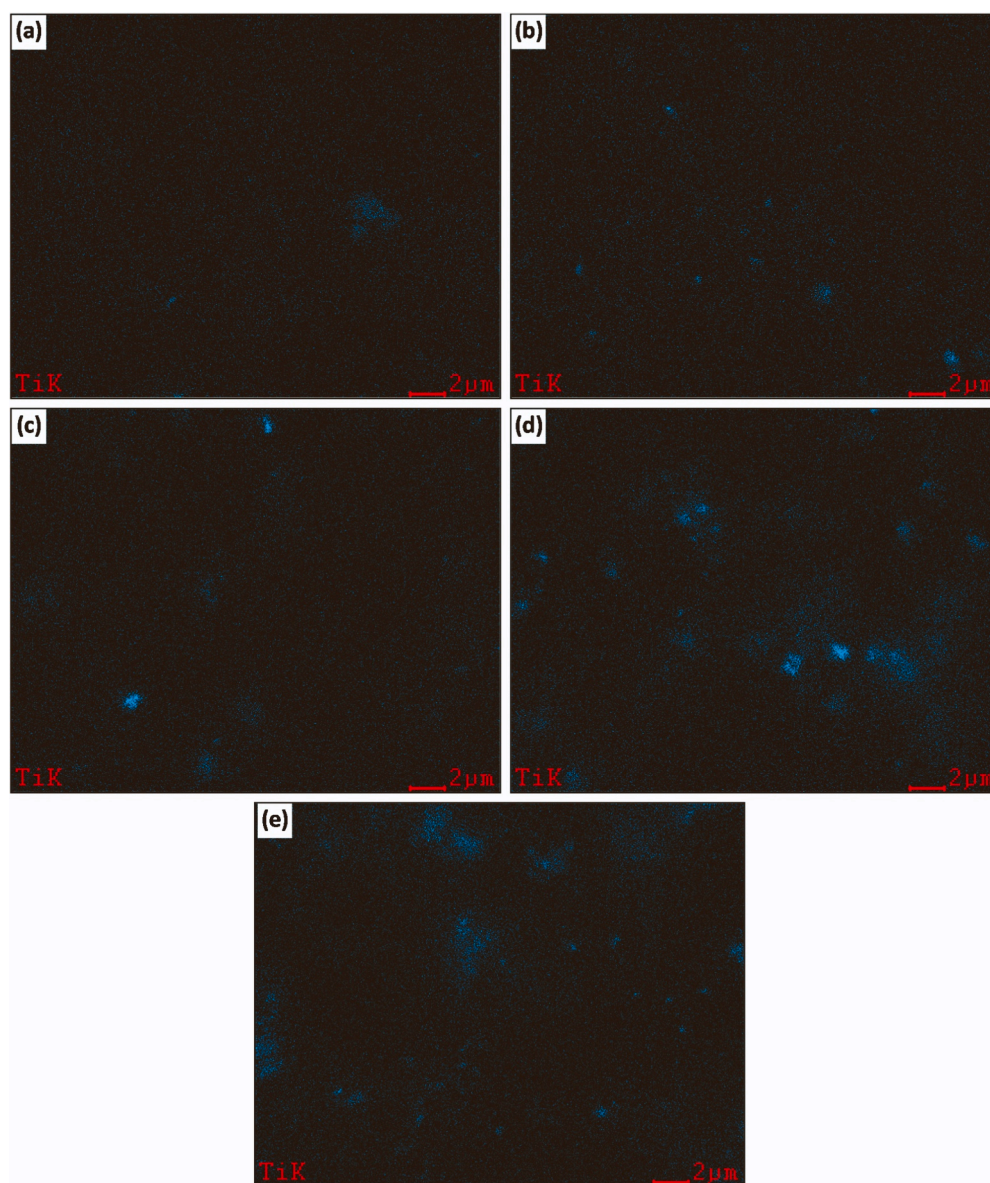


**Fig. A3.** EDX mapping of 3D printed/ $\text{TiO}_2$  composite resin materials showing the distribution of  $\text{TiO}_2$  NPs in: (a) 0.0 wt%, (b) 0.10 wt%, (c) 0.25 wt%, (d) 0.50 wt%, (e) 0.75 wt%.

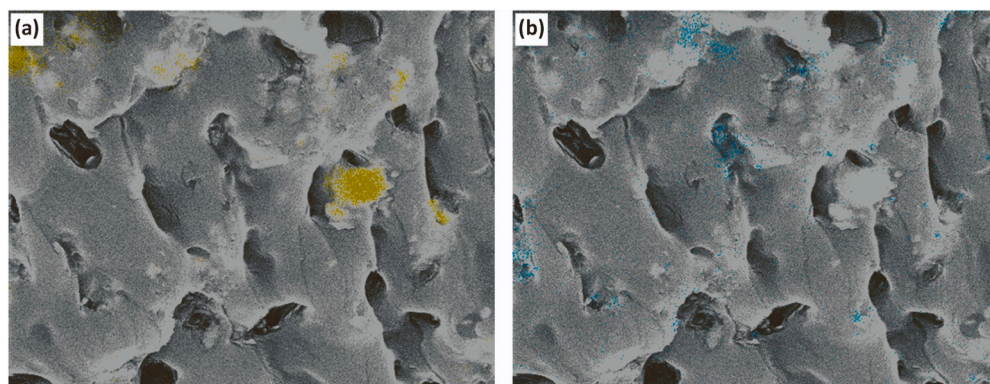


**Fig. A4.** EDX mapping of 3D printed/ $\text{TiO}_2$  nanocomposite with a concentration of 0.75 wt%  $\text{TiO}_2$  NPs at a magnification of 10 K 19 showing: (a)  $\text{SiO}_2$  fillers (yellow), (b)  $\text{TiO}_2$  fillers (cyan).





Fig. A5. Colours of specimens of 3D-printed/ TiO<sub>2</sub> NPs composite material with concentration of 0.0, 0.10, 0.25, 0.50, and 0.75 wt% from left to right.

Table A4

EDX analysis showing the amount of TiO<sub>2</sub> NPs by weight within each group before and after ageing in artificial saliva for 3 months.

Groups	TiO <sub>2</sub> (wt%) before ageing	TiO <sub>2</sub> (wt%) after ageing
A	0.04	N/A
B	0.11	0.06
C	0.25	0.20
D	0.43	0.36
E	0.96	0.40

## References

- Slade G, Akinkugbe A, Sanders A. Projections of US edentulism prevalence following 5 decades of decline. *J Dent Res* 2014;93(10):959–65.
- Cooper LF. The current and future treatment of edentulism. *J Prosthodont: Implant, Esthet Reconstr Dent* 2009;18(2):116–22.
- Al-Rafee MA. The epidemiology of edentulism and the associated factors: a literature review. *J Fam Med Prim Care* 2020;9(4):1841.
- Lee DJ, Saponaro PC. Management of edentulous patients. *Dent Clin* 2019;63(2):249–61.
- Anadioti E, Musharbash L, Blatz MB, Papavasiliou G, Kamposiora P. 3D printed complete removable dental prostheses: a narrative review. *BMC Oral Health* 2020;20(1):343.
- R. Diwan, Materials prescribed in the management of edentulous patients. *Prosthodontic Treatment for Edentulous Patients* ed. 2004;12:190–207.
- Zafar MS. Prosthodontic applications of polymethyl methacrylate (PMMA): an update. *Polymers* 2020;12(10):2299.
- Alla R, Raghavendra K, Vyas R, Konakanchi A. Conventional and contemporary polymers for the fabrication of denture prosthesis: part I—overview, composition and properties. *Int J Appl Dent Sci* 2015;1(4):82–9.
- Gautam R, Singh RD, Sharma VP, Siddhartha R, Chand P, Kumar R. Biocompatibility of polymethylmethacrylate resins used in dentistry. *J Biomed Mater Res Part B: Appl Biomater* 2012;100(5):1444–50.
- Gad MM, Rahoma A, Al-Thobity AM, ArRejaie AS. Influence of incorporation of ZrO<sub>2</sub> nanoparticles on the repair strength of polymethyl methacrylate denture bases. *Int J Nanomed* 2016;11:5633.
- Gad MM, Fouda SM, Al-Harbi FA, Napankangas R, Raustia A. PMMA denture base material enhancement: a review of fiber, filler, and nanofiller addition. *Int J Nanomed* 2017;12:3801–12.
- Chaijareenont P, Takahashi H, Nishiyama N, Arksornnukit M. Effect of different amounts of 3-methacryloxypropyltrimethoxysilane on the flexural properties and wear resistance of alumina reinforced PMMA. *Dent Mater J* 2012;31(4):623–8.
- Jordan J, Jacob KI, Tannenbaum R, Sharaf MA, Jasiuk I. Experimental trends in polymer nanocomposites—a review. *Mater Sci Eng: A* 2005;393(1–2):1–11.
- Ghahremani L, Shirkavand S, Akbari F, Sabzikari N. Tensile strength and impact strength of color modified acrylic resin reinforced with titanium dioxide nanoparticles. *J Clin Exp Dent* 2017;9(5):e661–5.
- Khaled S, Sui R, Charpentier PA, Rizkalla AS. Synthesis of TiO<sub>2</sub>–PMMA nanocomposite: using methacrylic acid as a coupling agent. *Langmuir* 2007;23(7):3988–95.
- Li F, Zhou S, You B, Wu L. Kinetic study on the UV-induced photopolymerization of epoxy acrylate/TiO<sub>2</sub> nanocomposites by FTIR spectroscopy. *J Appl Polym Sci* 2006;99(6):3281–7.
- Pazokifard S, Farrokhpay S, Mirabedini M, Esfandeh M. Surface treatment of tio2 nanoparticles via sol–gel method: effect of silane type on hydrophobicity of the nanoparticles. *Prog Org Coat* 2015;87:36–44.
- Chatterjee A. Properties improvement of PMMA using nano TiO<sub>2</sub>. *J Appl Polym Sci* 2010;118(5):2890–7.
- Reijnders L. The release of TiO<sub>2</sub> and SiO<sub>2</sub> nanoparticles from nanocomposites. *Polym Degrad Stab* 2009;94(5):873–6.
- Dawood A, Marti Marti B, Sauret-Jackson V, Darwood A. 3D printing in dentistry. *Br Dent J* 2015;219(11):521–9.
- Kessler A, Hickel R, Reyms M. 3D printing in dentistry—state of the art. *Oper Dent* 2020;45(1):30–40.
- Cristache CM, Totu EE, Iorgulescu G, Pantazi A, Dorobantu D, Nechifor AC, et al. Eighteen months follow-up with patient-centered outcomes assessment of complete dentures manufactured using a hybrid nanocomposite and additive CAD/CAM protocol. *J Clin Med* 2020;9(2).
- Lee S, Hong SJ, Paek J, Pae A, Kwon KR, Noh K. Comparing accuracy of denture bases fabricated by injection molding, CAD/CAM milling, and rapid prototyping method. *J Adv Prosthodont* 2019;11(1):55–64.
- Masri G, Mortada R, Ounsi H, Alharbi N, Boulous P, Salameh Z. Adaptation of complete denture base fabricated by conventional, milling, and 3-D printing techniques: an in vitro study. *J Conte Dent Pr* 2020;21(4):367–71.
- Alifui-Segbaya F, Bowman J, White AR, George R, Fidan I. Characterization of the double bond conversion of acrylic resins for 3D printing of dental prostheses. *Compendium* 2019;40(10).
- Lee J. Impact strength of 3D printed and conventional heat-cured and cold-cured denture base acrylics: The University of Texas School of Dentistry at Houston; 2020.
- Perea-Lowery L, Gibreel M, Vallittu PK, Lassila LV. 3D-printed vs. heat-polymerizing and autopolymerizing denture base acrylic resins. *Materials* 2021;14(19):5781.
- Gad MM, Fouda SM, Abualsaud R, Alshahrani FA, Al-Thobity AM, Khan SQ, et al. Strength and surface properties of a 3D-printed denture base polymer. *J Prosthodont* 2022;31(5):412–8.
- Aati S, Akram Z, Ngo H, Fawzy AS. Development of 3D printed resin reinforced with modified ZrO<sub>2</sub> nanoparticles for long-term provisional dental restorations. *Dent Mater* 2021;37(6):e360–74.
- Mubarak S, Dhamodharan D B, Kale M, Divakaran N, Senthil T, Wu L, et al. A novel approach to enhance mechanical and thermal properties of SLA 3D printed structure by incorporation of metal–metal oxide nanoparticles. *Nanomaterials* 2020;10(2):217.
- Chen S, Yang J, Jia YG, Lu B, Ren L. A Study of 3D-printable reinforced composite resin: PMMA modified with silver nanoparticles loaded cellulose nanocrystal. *Mater* 2018;11(12).
- Gad MM, Al-Harbi FA, Akhtar S, Fouda SM. 3D-printable denture base resin containing SiO<sub>2</sub> nanoparticles: an in vitro analysis of mechanical and surface properties. *J Prosthodont* 2022.
- Altarazi A, Haider J, Alhotan A, Silikas N, Devlin H. Assessing the physical and mechanical properties of 3D printed acrylic material for denture base application. *Dent Mater* 2022;38(12):1841–54.
- Bangera MK, Kotian R, Ravishankar N. Effect of titanium dioxide nanoparticle reinforcement on flexural strength of denture base resin: a systematic review and meta-analysis. *Jpn Dent Sci Rev* 2020;56(1):68–76.
- Hamming LM, Qiao R, Messersmith PB, Brinson LC. Effects of dispersion and interfacial modification on the macroscale properties of TiO<sub>2</sub> polymer–matrix nanocomposites. *Compos Sci Technol* 2009;69(11–12):1880–6.
- Gad MM, Abualsaud R. Behavior of PMMA denture base materials containing titanium dioxide nanoparticles: a literature review. *Int J Biomater* 2019.
- De Palma R, Peeters S, Van Bael MJ, Van den Rul H, Bonroy K, Laureyn W, et al. Silane ligand exchange to make hydrophobic superparamagnetic nanoparticles water-dispersible. *Chem Mater* 2007;19(7):1821–31.
- Frankamp BL, Fischer NO, Hong R, Srivastava S, Rotello VM. Surface modification using cubic silsesquioxane ligands. Facile synthesis of water-soluble metal oxide nanoparticles. *Chem Mater* 2006;18(4):956–9.
- Alshaikh AA, Khattar A, Almindil IA, Alsaiif MH, Akhtar S, Khan SQ, et al. 3D-printed nanocomposite denture-base resins: effect of ZrO<sub>2</sub> nanoparticles on the mechanical and surface properties in vitro. *Nanomaterials* 2022;12(14):2451.
- Totu EE, Nechifor AC, Nechifor G, Aboul-Enein HY, Cristache CM. Poly(methyl methacrylate) with TiO<sub>2</sub> nanoparticles inclusion for stereolithographic complete

- denture manufacturing - the future in dental care for elderly edentulous patients? *J Dent* 2017;59:68–77.
- [41] Chen SG, Yang JZ, Jia YG, Lu BH, Ren L. TiO<sub>2</sub> and PEEK reinforced 3D printing PMMA composite resin for dental denture base applications. *Nanomaterials* 2019;9(7).
- [42] Al-Dwairi ZN, Al Haj Ebrahim AA, Baba NZ. A comparison of the surface and mechanical properties of 3D printable denture-base resin material and conventional polymethylmethacrylate (PMMA). *J Prosthodont* 2023;32(1):40–8.
- [43] Aati S, Akram Z, Shrestha B, Patel J, Shih B, Shearston K, et al. Effect of post-curing light exposure time on the physico-mechanical properties and cytotoxicity of 3D-printed denture base material. *Dent Mater* 2022;38(1):57–67.
- [44] Greil V, Mayinger F, Reymus M, Stawarczyk B. Water sorption, water solubility, degree of conversion, elastic indentation modulus, edge chipping resistance and flexural strength of 3D-printed denture base resins. *J Mech Behav Biomed* 2023; 137:105565.
- [45] Mangal U, Seo JY, Yu J, Kwon JS, Choi SH. Incorporating aminated nanodiamonds to improve the mechanical properties of 3d-printed resin-based biomedical appliances. *Nanomaterials* 2020;10(5).
- [46] Sodagar A, Bahador A, Khalil S, Shahrودي AS, Kassaei MZ. The effect of TiO<sub>2</sub> and SiO<sub>2</sub> nanoparticles on flexural strength of poly (methyl methacrylate) acrylic resins. *J Prosthodont Res* 2013;57(1):15–9.
- [47] Ahmed MA, El-Shennawy M, Althomali YM, Omar AA. Effect of titanium dioxide nano particles incorporation on mechanical and physical properties on two different types of acrylic resin denture base. *World J Nano Sci Eng* 2016;6(3): 111–9.
- [48] Faot F, Costa MA. Impact strength and fracture morphology of denture acrylic resins. *J Prosthet Dent* 2006;96(5):367–73.
- [49] Mosalman S, Rashahmadi S, Hasanzadeh R. The effect of TiO<sub>2</sub> nanoparticles on mechanical properties of poly methyl methacrylate nanocomposites. *Int J Eng-Iran* 2017;30(5):807–13.
- [50] Prpic V, Schauperl Z, Catic A, Dulcic N, Cimic S. Comparison of mechanical properties of 3D-printed, CAD/CAM, and conventional denture base materials. *J Prosthodont* 2020;29(6):524–8.
- [51] Harini P, Mohamed K, Padmanabhan TV. Effect of Titanium dioxide nanoparticles on the flexural strength of polymethylmethacrylate: an in vitro study. *Indian J Dent Res* 2014;25(4):459–63.
- [52] Hashem M, Rez MFA, Fouad H, Elsarnagawy T, Elsharawy MA, Umar A, et al. Influence of titanium oxide nanoparticles on the physical and thermomechanical behavior of poly methyl methacrylate (PMMA): a denture base resin. *Sci Adv Mater* 2017;9(6):938–44.
- [53] Doğan A, Bek B, Cevik N, Usanmaz A. The effect of preparation conditions of acrylic denture base materials on the level of residual monomer, mechanical properties and water absorption. *J Dent* 1995;23(5):313–8.
- [54] Garcia LdFR, Roselino LdMR, Mundim FM, Pires-de-Souza FdCP, Consani S. Influence of artificial accelerated aging on dimensional stability of acrylic resins submitted to different storage protocols. *J Prosthodont: Implant, Esthet Reconstr Dent* 2010;19(6):432–7.
- [55] Wong DM, Cheng LY, Chow T, Clark RK. Effect of processing method on the dimensional accuracy and water sorption of acrylic resin dentures. *J Prosthet Dent* 1999;81(3):300–4.
- [56] Bartoloni J, Murchison D, Wofford D, Sarkar N. Degree of conversion in denture base materials for varied polymerization techniques 1. *J Oral Rehabil* 2000;27(6): 488–93.
- [57] Asmussen E, Peutzfeldt A. Influence of UEDMA, BisGMA and TEGDMA on selected mechanical properties of experimental resin composites. *Dent Mater* 1998;14(1): 51–6.
- [58] Ilie N, Hickel R. Investigations on mechanical behaviour of dental composites. *Clin Oral Investig* 2009;13:427–38.
- [59] Saini R, Kotian R, Madhyastha P, Srikant N. Comparative study of sorption and solubility of heat-cure and self-cure acrylic resins in different solutions. *Indian J Dent Res* 2016;27(3):288.
- [60] Polat TN, Karacaer Ö, Tezvergil A, Lassila LV, Vallittu PK. Water sorption, solubility and dimensional changes of denture base polymers reinforced with short glass fibers. *J Biomater Appl* 2003;17(4):321–35.
- [61] Ghavami-Lahiji M, Firouzmanesh M, Bagheri H, Kashi TSJ, Razazpour F, Behroozibakhsh M. The effect of thermocycling on the degree of conversion and mechanical properties of a microhybrid dental resin composite. *Restor Dent Endod* 2018;43(2).
- [62] Imazato S, Tarumi H, Kato S, Ebi N, Ehara A, Ebisu S. Water sorption, degree of conversion, and hydrophobicity of resins containing Bis-GMA and TEGDMA. *Dent Mater J* 1999;18(1):124–32.
- [63] Ferracane J, Berge H, Condon J. In vitro aging of dental composites in water—effect of degree of conversion, filler volume, and filler/matrix coupling. *J Biomed Mater Res: J Soc Biomater, Jpn Soc Biomater, Aust Soc Biomater* 1998;42 (3):465–72.
- [64] Tuna SH, Keyf F, Gumus HO, Uzun C. The evaluation of water sorption/solubility on various acrylic resins. *Eur J Dent* 2008;2(03):191–7.
- [65] Cucci ALM, Vergani CE, Giampaolo ET, Afonso MCdSF. Water sorption, solubility, and bond strength of two autopolymerizing acrylic resins and one heat-polymerizing acrylic resin. *J Prosthet Dent* 1998;80(4):434–8.